Structural Trends in First-Row Transition-Metal Bis(benzimidazole) Complexes†

Pramatha Payra, Huichang Zhang, Wai Him Kwok, Maosheng Duan, Judith Gallucci, and Michael K. Chan*

Departments of Chemistry and Biochemistry, The Ohio State University, 100 West 18th Avenue, Columbus, Ohio 43210

Received September 8, 1999

Dimethyl-substituted bis(benzimidazole) (Me_2BBZ) is a novel macrocyclic ligand that possesses an intrinsic nonplanarity. To examine how metal-ion binding affects the magnitude of this nonplanarity, we have determined the structures of a periodic series of Me_2BBZ complexes bound to Mn(II), Fe(II), Co(II), Ni(II), and Cu(II). These studies demonstrate that the extent of ligand ruffling and metal doming is indeed influenced by the nature of the metal. Concomitant with the periodic decrease of the ionic radii of the encapsulated divalent metal ion, a decrease in the magnitude of both the ligand nonplanarity and the metal out-of-the-plane distance is observed. For the metal out-of-the-plane distance, this correlation persists until the metal finally moves into the mean ligand plane. For the nonplanar distortion, the extent of the nonplanarity decreases to a limiting value that is intrinsic to the Me_2BBZ ligand due to steric factors. These observations indicate that the relative sizes of the metal ion and the Me_2BBZ ligand cavity have profound effects on the structural features of the metal−ligand complex.

Introduction

In metalloporphyrins, the conformation of the porphyrin ligand has been shown to influence their axial bonding affinities,[1] redox potentials,[2] electron-transfer rates,[3,4] and photophysical properties.[5−7] Indeed, nonplanar distortions of heme cofactors in proteins are thought to be important for tuning their functional properties, suggesting that similar features might be used to optimize the properties of synthetic tetrapyrroles for practical applications in photodynamic therapy,[8] biomimetic solar energy conversion,[9] and catalysis.[10] Hence, studies of the general factors that influence the nonplanarity of porphyrins and related ligands are of interest.

We recently completed the synthesis of a new class of porphyrin analogue, the dimethyl-substituted bis(benzimidazole) ligand (Me_2BBZ), and its manganese complex (Mn-Me_2BBZ).[11] Structures of both the diprotonated Me_2BBZ ligand, $[H_2(Me_2BBZ)](ClO_4)_2$ (**1**), and the Mn-Me_2BBZ complex, $[Mn(Me_2BBZ)Cl]Cl$ (**2**), revealed an inherent ruffling of the ligand resulting from its distinct steric and geometric features.[11] As a consequence of this ruffling, significant metal-doming of the Mn-Me_2BBZ complex was also observed.

Comparison of the diprotonated Me_2BBZ ligand and Mn-Me_2BBZ complex revealed differences in the magnitude of their nonplanarities. On the basis of the distances of the ligand atoms from the mean plane of the four-liganding nitrogens (N_4-plane), the Mn-Me_2BBZ complex appears less distorted. Each of the out-of-plane distances of the ligand atoms in the Mn-Me_2BBZ complex is smaller than in the diprotonated Me_2BBZ ligand. These features are important since they demonstrate that the observed nonplanarity is an inherent feature of the Me_2BBZ ligand and that the metal ion can modulate the magnitude of this nonplanarity.

To evaluate the extent to which metals modulate the ligand ruffling in metal Me_2BBZ complexes, and to elucidate the mechanism by which this control is achieved, we have synthesized (Scheme 1) and crystallographically characterized four related metal-Me_2BBZ complexes: $[Fe(Me_2BBZ)Cl](BPh_4)$, (Fe-Me_2BBZ, **3**), $[Co(Me_2BBZ)Cl]Cl$, (Co-Me_2BBZ, **4**), $[[Ni(Me_2BBZ)(H_2O)(CH_3CN)][Ni(Me_2BBZ)(H_2O)_2](ClO_4)_4$, (Ni-$Me_2BBZ$, **5**), and $[Cu(Me_2BBZ)(ClO_4)_2]$, (Cu-Me_2BBZ, **6**). Structural comparison of these complexes along with the Mn-Me_2BBZ complex yields insight into the structural features that control metal−bis(benzimidazole) geometries.

* To whom correspondence should be addressed. Telephone: 614-292-8375. Fax: 614-292-6773. E-mail: chan@chemistry.ohio-state.edu.

† Abbreviations used: Me_2BBZ, dimethyl-substituted bis(benzimidazole) ligand; Mn-Me_2BBZ, manganese(II) Me_2BBZ complex; Fe-Me_2BBZ, iron(II) Me_2BBZ complex; Co-Me_2BBZ, cobalt(II) Me_2BBZ complex; Ni-Me_2BBZ, nickel(II) Me_2BBZ complex; Cu-Me_2BBZ, copper(II) Me_2BBZ complex; TPP, tetraphenylporphyrin; $TP_{piv}P$, *meso*-5,10,15,20-tetrakis(*o*-pivalamidophenyl)porphyrin; OEP, octaethylporphyrin; DMAP, 4-(dimethylamino)pyridine; $F_{28}TPP$, 2,3,7,8,12,13,17,18-octafluoro-5,10,15,20-tetrakis(pentafluorophenyl)porphyrin; py, pyridine; $TPP(Br)_4(CN)_4$, 2,3,12,13-tetrabromo-7,8,17,18-tetracyano-5,10,15,20-tetraphenylporphyrin; $TPP(CN)_4$, 7,8,17,18-tetracyano-5,10,15,20-tetraphenylporphyrin; OETPP, 2,3,7,8,12,13,17,18-octaethyl-5,10,15,20-tetraphenylporphyrin.

(1) David, S.; James, B. R.; Dolphin, D.; Traylor, T. G.; Lopez, M. A. *J. Am. Chem. Soc.* **1994**, *116*, 6−14.
(2) Barkigia, K. M.; Chantranupong, L.; Smith, K. M.; Fajer, J. *J. Am. Chem. Soc.* **1988**, *110*, 7566−7567.
(3) Hobbs, J. D.; Shelnutt, J. A. *J. Protein Chem.* **1995**, *14*, 19−25.
(4) Fukuzumi, S.; Nakanishi, I.; Barbe, J.-M.; Guilard, R.; Van Caemelbecke, E.; Guo, N.; Kadish, K. M. *Angew. Chem., Int. Ed. Engl.* **1999**, *38*, 964−966.
(5) Medforth, C. J.; Berber, M. D.; Smith, K. M. *Tetrahedron Lett.* **1990**, *31*, 3719−3722.
(6) Shelnutt, J. A.; Medforth, C. J.; Berber, M. D.; Barkigia, K. M.; Smith, K. M. *J. Am. Chem. Soc.* **1991**, *113*, 4077−4087.
(7) Gentemann, S.; Medforth, C. J.; Ema, T.; Nelson, N. Y.; Smith, K. M.; Fajer, J.; Holten, D. *Chem. Phys. Lett.* **1995**, *245*, 441−447.
(8) Grossweiner, L. I. *Photodynamic therapy with porphyrin derivatives*; Duke, S. O., Rebeiz, C. A., Eds.; American Chemical Society: Washington, DC, 1994; Vol. 559, pp 255−65.
(9) Lindsey, J. S. *Modular design of multiporphyrin arrays for studies in photosynthesis and molecular photonics*; Michi, J., Ed.; Kluwer Academic Publishers: Dordrecht, The Netherlands, 1997; Vol. 499, pp 517−528.
(10) Collman, J. P.; Zhang, X.; Lee, V. J.; Uffelman, E. S.; Brauman, J. I. *Science* **1993**, *261*, 1404−1411.
(11) Kwok, W. H.; Zhang, H.; Payra, P.; Duan, M.; Hung, S.-C.; Johnston, D. H.; Gallucci, J.; Skrzypczak-Jankun, E.; Chan, M. K. Submitted for publication.

10.1021/ic991075a CCC: $19.00
Published on Web 02/25/2000

Scheme 1

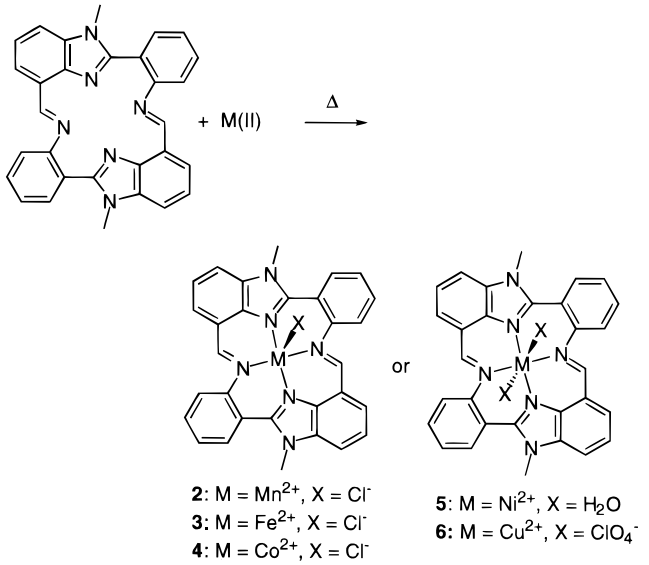

Experimental Section

Safety Note. *Caution! Perchlorate salts of metal complexes with organic ligands are potentially explosive. Only small amounts of these materials should be prepared, and they should be handled with great caution.*

General Methods. Unless stated otherwise, all materials were obtained from commercial suppliers and used without further purification. Silica gel (Scientific Adsorbents Inc. 32-63 U, 40 μm) was used for column chromatography. All compounds were fully characterized by elemental analysis and infrared and UV−visible spectroscopies. Infrared spectra were recorded on a Perkin-Elmer 16 PC FT-IR instrument. UV−visible spectra were measured using a Perkin-Elmer model Lambda 20 UV−visible spectrophotometer. The Me_2BBZ ligand was synthesized as reported previously.[11]

Crystal Structure Determinations. The details of the structure determination and refinement for the reported structures are provided as Supporting Information. While the Fe-Me_2BBZ, Co-Me_2BBZ, and Cu-Me_2BBZ structures contain one molecule in the asymmetric unit, the Ni-Me_2BBZ structure contains two molecules (A and B). The two Ni-Me_2BBZ molecules are similar except that molecule A has an acetonitrile and a water molecule as axial ligands, while molecule B has two bound water molecules.

[Fe(Me_2BBZ)Cl](BPh_4) (3). A red-colored solution was obtained by refluxing the Me_2BBZ ligand (0.50 g, 0.93 mmol) with $FeCl_2 \cdot 4H_2O$ (0.18 g, 0.93 mmol) in CH_3CN for 20 h under nitrogen. The solvent was removed in vacuo, and the resulting red solid was dissolved in 50 mL of degassed MeOH. Addition of $NaBPh_4$ (0.31 g, 0.93 mmol) to the solution yielded a brick-red solid upon stirring for 15 min. Recrystallization from acetonitrile affords a dark brown solid (0.79 g, 85%). Crystals suitable for X-ray analysis were obtained by slow diffusion of pentane into an acetonitrile solution of the complex at −7 °C over a period of 3 days. Anal. Calcd for [Fe(Me_2BBZ)Cl](BPh_4), $C_{54}H_{42}N_6BClFe$: C, 73.96; H, 4.79; N, 9.58. Found: C, 73.69; H, 4.76; N, 9.64. UV−visible spectrum (λ (ϵ, M^{-1} cm^{-1}) in CH_3CN): 243 (2.17 × 10^4), 328 (1.36 × 10^4). IR (KBr, cm^{-1}): 1658 w, 1609 m, 1569 m, 1519 w, 1473 s, 1427 m, 1379 m, 1222 w, 1065 w, 1030 w, 848 w, 810 w, 734 s, 704 vs, 611 m.

[Co(Me_2BBZ)Cl]Cl (4). The Me_2BBZ ligand (0.201 g, 0.43 mmol) was reacted with $CoCl_2 \cdot 6H_2O$ (0.13 g, 0.43 mmol) in CH_3CN. An orange red mixture was obtained upon stirring. The solution was refluxed for 20 h, and the solvent was removed by rotary evaporation. The crude product was purified by column chromatography (CH_2Cl_2:hexane:MeOH = 3:1:1) and dried to give an orange solid (0.201 g, 67.5% yield). Crystals suitable for X-ray analysis were obtained by slow diffusion of pentane into a methanol solution over 7 days at −7 °C. Anal. Calcd for [Co(Me_2BBZ)Cl]Cl, $C_{30}H_{22}N_6Cl_2Co$: C, 60.42; H, 3.69, N 14.09. Found: C, 59.92; H, 3.83; N, 13.85. UV−visible spectrum (λ (ϵ, M^{-1} cm^{-1}) in CH_3CN): 242 (2.76 × 10^4), 328 (2.92 × 10^4). IR (KBr, cm^{-1}): 1611 s, 1570 s, 1518 w, 1473 vs, 1429 m, 1379 m, 1301 w, 1222 m, 1189 m, 1120 w, 1066 w, 921 w, 849 w, 798 w, 753 s, 715 w, 590 w.

[Ni(Me_2BBZ)(H_2O)$_2$](ClO_4)$_2$ (5). The Me_2BBZ ligand (0.49 g, 0.96 mmol) was reacted with $Ni(ClO_4)_2$ (0.348 g, 0.96 mmol) in CH_3CN. The color of the solution changed from green to orange upon stirring. The solution was refluxed for 20 h, and the solvent was removed by rotary evaporation. The crude product was purified by column chromatography using CH_3CN as the eluent and dried to give an orange solid (0.55 g, 69% yield). Crystals suitable for X-ray analysis were obtained by slow diffusion of hexane into an acetonitrile solution over 7 days at −7 °C. Anal. Calcd for [Ni(Me_2BBZ)(H_2O)$_2$](ClO_4)$_2$, $C_{30}H_{26}N_6O_{10}Cl_2Ni$: C, 47.39; H, 3.42; N, 11.05; Cl, 9.33. Found: C, 47.25; H, 3.60; N, 10.85; Cl, 9.44. UV−visible spectrum (λ (ϵ, M^{-1}

Table 1. Crystallographic Data for [Fe(Me_2BBZ)Cl](BPh_4)·$3CH_3CN$ (**3**), [Co(Me_2BBZ)Cl]Cl·$3CH_3OH$ (**4**), [Ni(Me_2BBZ)(H_2O)(CH_3CN)][Ni(Me_2BBZ)(H_2O)$_2$](ClO_4)$_4$·$6CH_3CN$ (**5**), and [Cu(Me_2BBZ)(ClO_4)$_2$] (**6**)

	complex no.			
	3	**4**	**5**	**6**
formula	$C_{60}H_{51}BClFeN_9$	$C_{33}H_{34}Cl_2CoN_6O_3$	$C_{74}H_{71}Cl_4Ni_2N_{19}O_{19}$	$C_{30}H_{22}Cl_2CuN_6O_8$
fw	1000.21	692.49	1789.72	728.98
temp, K	173	223	213	193
cryst system	triclinic	triclinic	monoclinic	monoclinic
space group	$P\bar{1}$	$P\bar{1}$	$P2_1/c$	$P2_1/n$
a, Å	13.0776(3)	10.553(1)	17.710(4)	14.1489(2)
b, Å	13.3976(2)	11.193(2)	21.293(4)	13.3826(2)
c, Å	15.5236(3)	15.510(2)	21.814(3)	15.9805(2)
α, deg	72.086(1)	110.44(1)		
β, deg	75.900(1)	92.03(1)	106.740(12)	106.575(1)
γ, deg	84.375(1)	110.260(9)		
Z, formula unit	2	2	4	4
V, Å^3	2509.25(8)	1584.8(4)	7877(2)	2900.16(7)
d_{calcd}, g·cm^{-3}	1.324	1.451	1.509	1.670
μ_{calcd}, mm^{-1}	0.404	0.755	0.698	1.003
no. of data collcd	51606	7731	10753	59885
no. of unique data (all)	8859	7330	10359	6649
no. of variable params	655	407	1051	426
R_1,[a] wR_2[b] (2σ)	0.044, 0.086	0.051, 0.131	0.071, 0.169	0.043, 0.115
R_1,[a] wR_2[b] (all data)	0.074, 0.099	0.110, 0.160	0.219, 0.231	0.053, 0.121
gof on F^2 (all data)	1.06	1.311	1.034	1.037

[a] $R_1 = \sum||F_o| - |F_c||/\sum|F_o|$. [b] $wR_2(F^2) = [\sum w(F_o^2 - F_c^2)^2/\sum w(F_o^2)^2]^{1/2}$.

Table 2. Selected Bond Distances (Å) and Angles (deg) for [Fe(Me$_2$BBZ)Cl](BPh$_4$) (**3**)

Fe−N(1)	2.057(2)	Fe−N(3)	2.049(2)
Fe−N(2)	2.203(2)	Fe−N(4)	2.198(2)
Fe−Cl	2.2508(7)		
N(1)−Fe−N(2)	81.89(8)	N(1)−Fe−N(3)	131.87(8)
N(1)−Fe−N(4)	85.75(8)	N(1)−Fe−Cl	114.65(6)
N(2)−Fe−N(3)	86.06(8)	N(2)−Fe−N(4)	150.03(8)
N(2)−Fe−Cl	105.97(6)	N(3)−Fe−N(4)	82.07(8)
N(3)−Fe−Cl	113.47(6)	N(4)−Fe−Cl	104.00(6)

Table 3. Selected Bond Distances (Å) and Angles (deg) for [Co(Me$_2$BBZ)Cl]Cl (**4**)

Co−N(1)	1.998(3)	Co−N(2)	2.169(3)
Co−N(3)	2.003(3)	Co−N(4)	2.194(3)
Co−Cl(1)	2.263(1)		
N(1)−Co−N(2)	84.4(1)	N(1)−Co−N(3)	138.2(1)
N(1)−Co−N(4)	88.5(1)	N(1)−Co−Cl(1)	113.13(8)
N(2)−Co−N(3)	88.3(1)	N(2)−Co−N(4)	160.2(1)
N(2)−Co−Cl(1)	98.51(8)	N(3)−Co−N(4)	84.8(1)
N(3)−Co−Cl(1)	108.61(8)	N(4)−Co−Cl(1)	101.31(8)

cm^{-1}) in CH$_3$CN): 242 (1.89×10^4), 333 (2.39×10^4). IR (KBr, cm^{-1}): 3450 s, br, 1611 s, 1569 s, 1525 w, 1485 vs, 1435 m, 1398 m, 1377 m, 1312 w, 1231 w, 1194 m, 1099 vs, br, 923 w, 852 w, 817 w, 799 w, 777 w, 757 s, 715 w, 625 s.

[Cu(Me$_2$BBZ)(ClO$_4$)$_2$] (6). The Me$_2$BBZ ligand (0.44 g, 0.82 mmol) was reacted with Cu(ClO$_4$)$_2$ (0.304 g, 0.82 mmol) in CH$_3$CN. The color of the solution changed from orange-red to yellow-orange color upon stirring. The solution was refluxed for 20 h, and the solvent was removed by rotary evaporation. The crude product was purified by column chromatography using CH$_3$CN as the eluent and dried to give a red solid (0.51 g, 75% yield). Crystals suitable for X-ray analysis were obtained by slow diffusion of hexane into an acetonitrile solution over 4 days at −7 °C. Anal. Calcd for [Cu(Me$_2$BBZ)(ClO$_4$)$_2$], $C_{30}H_{22}N_6O_8Cl_2Cu$: C, 49.41; H, 3.01; N, 11.52; Cl, 9.74. Found: C, 49.90; H, 3.04; N, 12.12; Cl, 9.17. UV−visible spectrum (λ (ϵ, M^{-1} cm^{-1}) in CH$_3$CN): 239 (2.64×10^4), 333 (2.93×10^4). IR (KBr, cm^{-1}): 1658 w, 1612 s, 1564 s, 1525 w, 1480 vs, 1435 m, 1383 m, 1315 w, 1291 w, 1251 w, 1230 w, 1194 w, 1094 vs, br, 927 w, 855 w, 817 w, 804 w, 777 w, 758 s, 713 w, 624 s.

Results and Discussion

A comparison of the structures of the Fe-Me$_2$BBZ, Co-Me$_2$BBZ, Ni-Me$_2$BBZ, and Cu-Me$_2$BBZ complexes reveals a general conservation of their geometric features (Tables 1−5, Figures 1−3). As in the Mn-Me$_2$BBZ complex, in each complex the Me$_2$BBZ ligand binds the metal along the equatorial plane with average metal−nitrogen bond distances comparable to those of divalent metalloporphyrins (Table 6[12−19]). Within a given metal−bis(benzimidazole), however, the average metal−N(imine) and metal−N(benzimidazole) bond lengths differ significantly (Table 7). Metal−N(benzimidazole) distances in metallobis(benzimidazole)s have values that are slightly shorter than the average metal−N bond length, while metal−N(imine) bond lengths are found to be slightly longer.

Another common feature in these complexes is the intrinsic nonplanarity of the Me$_2$BBZ ligand. While this is presumably due to common steric interactions, the extent of ruffling is found to differ between molecules—a feature that is manifested in the observed geometry at the metal center. The structures of the periodic series of metal Me$_2$BBZ complexes (Mn, Fe, Co, Ni, Cu) can be divided into two groups, those that are five-coordinate and exhibit significant metal doming (Mn, Fe, and Co) and those that adopt an octahedral or pseudooctahedral geometry and have little metal doming (Ni, Cu). As might be expected, the coordination number of the metal is highly

Table 4. Selected Bond Distances (Å) and Angles (deg) for [Ni(Me$_2$BBZ)(H$_2$O)(CH$_3$CN)][Ni(Me$_2$BBZ)(H$_2$O)$_2$](ClO$_4$)$_4$ (**5**)

Ni(1)−N(1A)	1.987(7)	Ni(1)−N(2A)	2.152(8)
Ni(1)−N(3A)	1.986(8)	Ni(1)−N(4A)	2.126(8)
Ni(1)−O(1A)	2.084(7)	Ni(1)−N(7A)	2.143(8)
Ni(2)−N(1B)	1.994(8)	Ni(2)−N(2B)	2.136(8)
Ni(2)−N(3B)	1.987(8)	Ni(2)−N(4B)	2.136(8)
Ni(2)−O(1B)	2.060(7)	Ni(2)−O(2B)	2.174(6)
N(1A)−Ni(1)−N(2A)	88.1(3)	N(1A)−Ni(1)−N(3A)	170.3(3)
N(1A)−Ni(1)−N(4A)	91.6(3)	N(1A)−Ni(1)−O(1A)	95.9(3)
N(1A)−Ni(1)−N(7A)	85.5(3)	N(2A)−Ni(1)−N(3A)	91.4(3)
N(2A)−Ni(1)−N(4A)	176.4(3)	N(2A)−Ni(1)−O(1A)	92.4(3)
N(2A)−Ni(1)−N(7A)	87.2(3)	N(3A)−Ni(1)−N(4A)	88.3(3)
N(3A)−Ni(1)−O(1A)	93.8(3)	N(3A)−Ni(1)−N(7A)	84.9(3)
N(4A)−Ni(1)−O(1A)	91.1(3)	N(4A)−Ni(1)−N(7A)	89.2(3)
O(1A)−Ni(1)−N(7A)	178.6(3)		
N(1B)−Ni(2)−N(2B)	87.8(3)	N(1B)−Ni(2)−N(3B)	168.7(3)
N(1B)−Ni(2)−N(4B)	91.7(3)	N(1B)−Ni(2)−O(1B)	94.9(3)
N(1B)−Ni(2)−O(2B)	83.6(3)	N(2B)−Ni(2)−N(3B)	92.1(3)
N(2B)−Ni(2)−N(4B)	176.6(3)	N(2B)−Ni(2)−O(1B)	91.5(3)
N(2B)−Ni(2)−O(2B)	88.0(3)	N(3B)−Ni(2)−N(4B)	87.7(3)
N(3B)−Ni(2)−O(1B)	96.4(3)	N(3B)−Ni(2)−O(2B)	85.1(3)
N(4B)−Ni(2)−O(1B)	91.9(3)	N(4B)−Ni(2)−O(2B)	88.6(3)
O(1B)−Ni(2)−O(2B)	178.4(3)		

Table 5. Selected Bond Distances (Å) and Angles (deg) for [Cu(Me$_2$BBZ)(ClO$_4$)$_2$] (**6**)

Cu−N(1)	1.928(2)	Cu−N(2)	2.068(2)
Cu−N(3)	1.925(2)	Cu−N(4)	2.054(2)
Cu−O(5)	2.352(2)	Cu···O(1)	2.744(2)
N(1)−Cu−N(2)	87.33(8)	N(1)−Cu−N(3)	166.28(9)
N(1)−Cu−N(4)	91.73(8)	N(1)−Cu−O(5)	106.43(8)
N(2)−Cu−N(3)	91.35(8)	N(2)−Cu−N(4)	173.40(8)
N(2)−Cu−O(5)	94.19(10)	N(3)−Cu−N(4)	88.02(8)
N(3)−Cu−O(5)	87.29(9)	N(4)−Cu−O(5)	92.34(10)

Table 6. Comparison of M−N Bond Lengths in Metal−Benzimidazoles and −Porphyrins

complex	av M−N bond dist, Å	ref
[Mn(Me$_2$BBz)Cl]$^+$	2.19(7)	11
[Mn(TPP)Cl]$^-$	2.16(1)	12
[Fe(Me$_2$BBz)Cl]$^+$	2.13(7)	this work
[Fe(TP$_{piv}$P)(2-MeIm)]$^-$	2.106(20)	13
[Fe(TP$_{piv}$P)(CH$_3$CO$_2$)]$^-$	2.107(14)	14
[Fe(TP$_{piv}$P)(OC$_6$H$_5$)]$^-$	2.114(2)	15
[Co(Me$_2$BBz)Cl]$^+$	2.09(9)	this work
[Co(OEP)(DMAP)]	1.982(2)	16
[Co(F$_{28}$TPP)·2tol]	1.986(1)	17
[Co(F$_{28}$TPP)·2THF]	2.068(2)	17
[Ni(Me$_2$BBz)(H$_2$O)$_2$]$^{2+}$	2.06(8)	this work
[Ni(TPP(Br)$_4$(CN)$_4$)(py)$_2$]	2.056(2)	18
[Ni(TPP(CN)$_4$)(1-MeIm)$_2$]	2.052(2)	18
[Cu(Me$_2$BBz)(ClO$_4$)$_2$]	1.99(7)	this work
[Cu(OETPP)]$^+$pyI$_3^-$·py	1.99(1)	19

(12) VanAtta, R. B.; Strouse, C. E.; Hanson, L. K.; Valentine, J. S. *J. Am. Chem. Soc.* **1987**, *109*, 1425−1434.
(13) Mandon, D.; Ott-Woelfel, F.; Fischer, J.; Weiss, R.; Bill, E.; Trautwein, A. X. *Inorg. Chem.* **1990**, *29*, 2442−2447.
(14) Bominaar, E. L.; Ding, X.-Q.; Gismelseed, A.; Bill, E.; Winkler, H.; Trautwein, A. X.; Nasri, H.; Fischer, J.; Weiss, R. *Inorg. Chem.* **1992**, *31*, 1845−1854.
(15) Nasri, H.; Fischer, J.; Weiss, R. *J. Am. Chem. Soc.* **1987**, *109*, 2549−2550.
(16) Summers, J. S.; Peterson, J. L.; Stolzenberg, A. M. *J. Am. Chem. Soc.* **1994**, *116*, 7189−7195.
(17) Smirnov, V. V.; Woller, E. K.; DiMagno, S. G. *Inorg. Chem.* **1998**, *37*, 4971−4978.
(18) Duval, H.; Bulach, V.; Fischer, J.; Weiss, R. *Inorg. Chem.* **1999**, *38*, 5495−5501.
(19) Renner, M. W.; Barkigia, K. M.; Fajer, J. *Inorg. Chim. Acta* **1997**, *263*, 181−187.

Table 7. Comparison of the Structures of Metal−Me_2BBZ Complexes

complex	M−N(benzimidazole) dist, Å	M−N(Schiff base) dist, Å	M-Cl dist, Å	out-of-plane metal dist, Å	dihedral angle 1[b] Ph−benzimidazole, deg	dihedral angle 2[c] Schiff base, deg
H_2-Me_2BBZ					49.17	53.69
Mn-Me_2BBZ	2.122(4)	2.267(10)	2.3186(10)	0.796	33.6	51.3
Fe-Me_2BBZ	2.053(4)	2.200(2)	2.2508(7)	0.704	34.6	51.7
Co-Me_2BBZ	2.000(3)	2.182(12)	2.263(1)	0.54	32.0	47.6
Ni-Me_2BBZ[a]	1.988(8)	2.137(8)	Ni−O (H_2O), 2.060(7), 2.174(6)	0.13	35.7	39.7
Cu-Me_2BBZ	1.926(2)	2.061(7)	Cu−O (ClO_4), 2.352(2), 2.744(2)	0.17	30.5	41.9

[a] Values are the average of the two molecules. [b] Average dihedral angle between the phenyl ring and benzimidazole plane for the two phenylbenzimidazole units within each complex (C(8)−C(13)−C(14)−N(3) and C(23)−C(28)−C(29)−N(1)). [c] Average dihedral angle located at the imine C−N bond for the two Schiff-base units within each complex (C(7)−N(4)−C(8)−C(9) and C(22)−N(2)−C(23)−C(24).

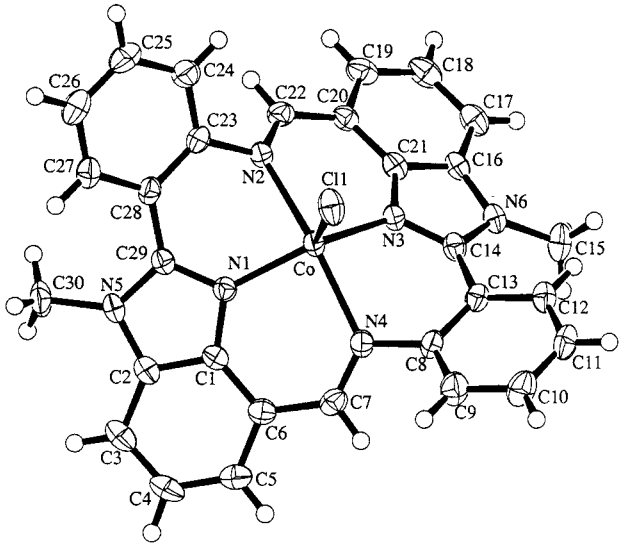

Figure 1. ORTEP diagram of [Co(Me_2BBZ)Cl]Cl. The structure of the Fe-Me_2BBZ complex is similar.

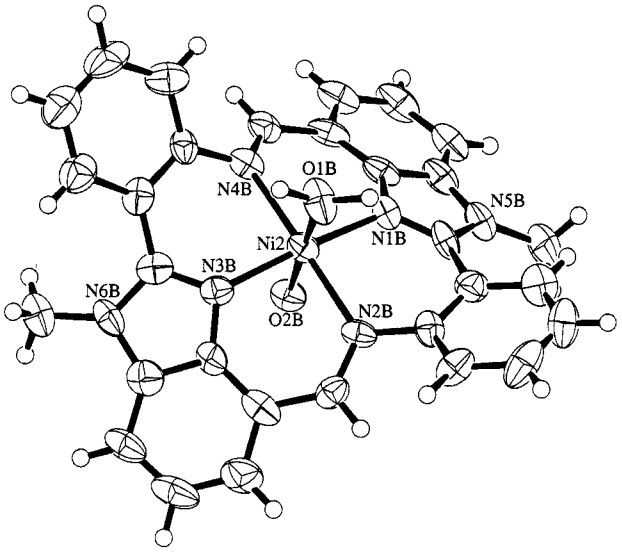

Figure 2. ORTEP diagram of [Ni(Me_2BBZ)(H_2O)$_2$](ClO_4)$_2$ (molecule B).

correlated with the distance of the metal from the N_4-plane (Table 7). Five-coordinate (Mn, Fe, Co) metal−Me_2BBZ complexes have larger out-of-plane distances than octahedral (Ni) and pseudooctahedral (Cu) complexes.

The out-of-plane metal distances decrease gradually on going from the left to right across the periodic table. This trend is consistent with the expected decrease in the ionic radii for the five divalent metals. Tabulation of the average metal−nitrogen bond distances reveals a distinct trend (Mn−N > Fe−N > Co−N > Ni−N > Cu−N) that appears strongly correlated with the out-of-plane metal distance. These results support the notion that the relative size of the metal ion to the Me_2BBZ metal binding pocket mediates the magnitude of metal doming. While nickel and copper ions are small enough to fit into the cavity, the three larger metals are not.

Further analysis reveals that these factors are also relevant to the nonplanarity of the Me_2BBZ ligand itself. One way to compare the extent of ruffling in Me_2BBZ complexes is to analyze the distances of the ligand atoms from the N_4-plane. A tabulation of these values, as shown in Figure 4, reveals a trend for the nonplanarities of metal Me_2BBZ complexes that coincides with the periodic trends in the atomic radii. Presumably as the size of the metal gets larger, it requires the metal to adopt a position above the mean ligand plane; which, in turn, induces the increased puckering of the ligand. Hence, to a first approximation, the geometry of metal Me_2BBZ complexes can be controlled by judicious choice of the metal ion.

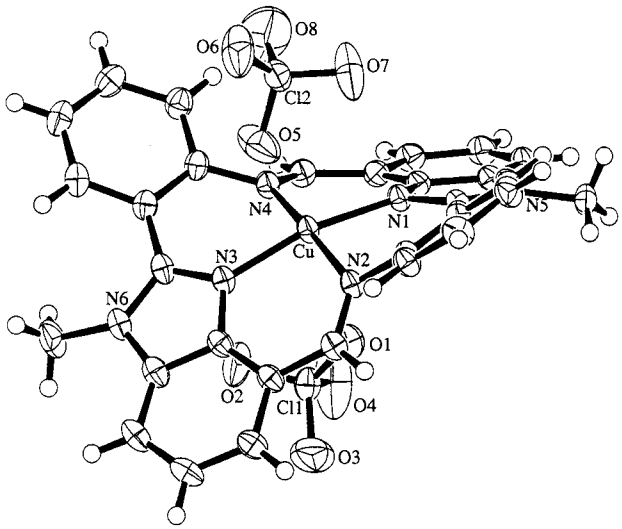

Figure 3. ORTEP diagram of [Cu(Me_2BBZ)(ClO_4)$_2$]

An alternative way to characterize the nonplanarity is to compare the dihedral angles localized between the benzimidazole and phenyl rings and along the imine carbon and nitrogen bond of the Schiff base. These results, shown in Table 7, reveal potential insight into the forces that alter the puckering of the ligand. Comparison of the phenyl−benzimidazole dihedral angle in this series of Me_2BBZ complexes reveals that this angle is

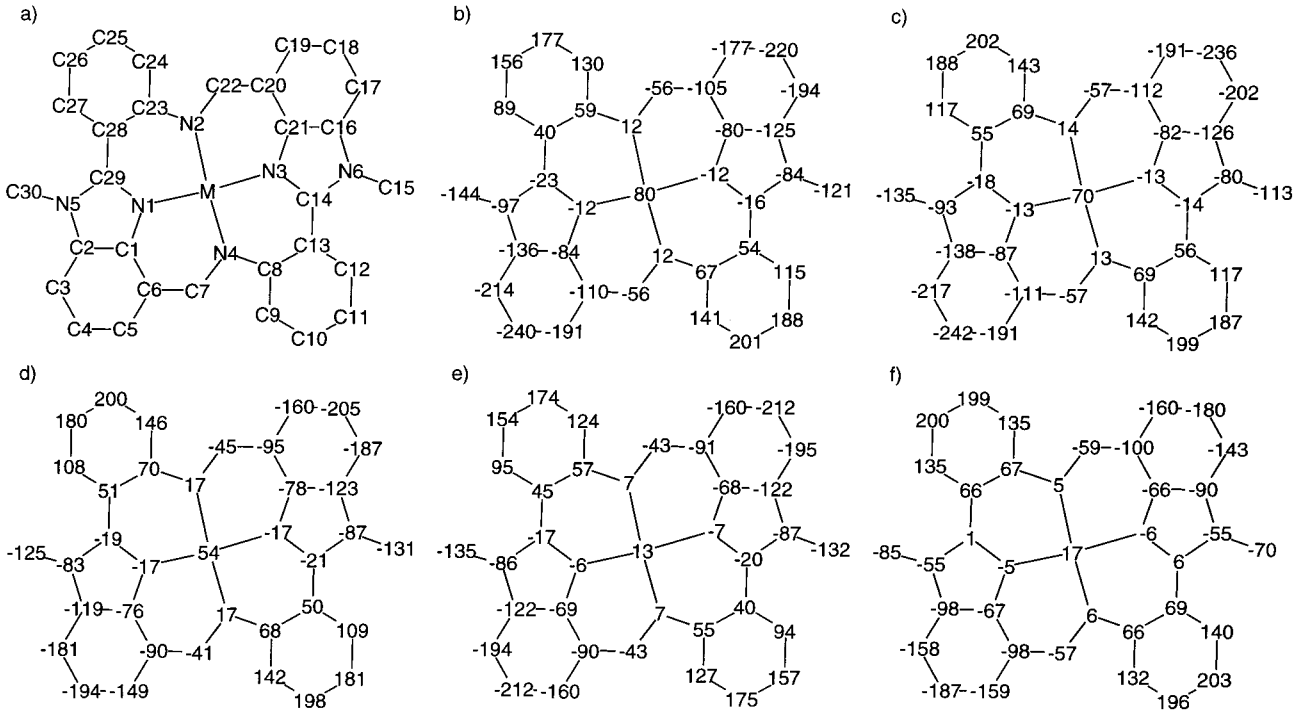

Figure 4. Formal diagram of the Me_2-bis(benzimidazole) cores depicting the perpendicular displacement of each unique atom from the mean plane of the four liganding nitrogens in units of 0.01 Å: (a) atom-labeling scheme; (b) Mn-Me_2BBZ (**2**);[11] (c) Fe-Me_2BBZ (**3**); (d) Co-Me_2BBZ (**4**); (e) Ni-Me_2BBZ (**5**); (f) Cu-Me_2BBZ (**6**).

independent of the type of metal but is influenced by the binding of the metal. While this angle is close to 33° for each of the five metal Me_2BBZ complexes, the simple diprotonated Me_2-BBZ ligand has a dihedral angle of almost 50°. These data suggest that the binding of metals serves to flatten the ligand along the metal-to-nitrogen(benzimidazole) bond.

Interestingly, very different trends are observed for the dihedral angles of the Schiff base. These dihedral angles exhibit a significant metal dependence, ranging from 40 to 52°, with values that correlate with the size of the metal radii (Table 7). As the sizes of the metal increases, the dihedral angle of the Schiff base increases accordingly. The binding of the metal itself, however, appears to have little effect on this dihedral angle. The diprotonated ligand, Mn-Me_2BBZ, and Fe-Me_2BBZ complexes have comparable values. These data strongly suggest that the metal-dependent nonplanar distortions of the Me_2BBZ ligand are localized at the Schiff base.

One other feature made apparent by this study is the existence of two distinct sides of the Me_2BBZ ligand—each of which has distinct ligand binding properties. Using the N_4-plane to distinguish these two sides, the phenyl groups are distorted to one side of the N_4-plane (defined to be above), while the benzimidazole groups are directed toward the other side of the N_4-plane (below). Using this nomenclature, in each of the pentacoordinate metal−Me_2BBZ structures, both the metal and the chloride ligand are found to lie above the N_4-plane. These tendencies are also manifested in the octahedral Ni-Me_2BBZ and pseudooctahedral Cu-Me_2BBZ complexes, although in a slightly different way. The metal-to-ligand bond lengths of the axial ligands above the N_4-plane are found to be significantly shorter than the bond lengths for the identical ligand below the N_4-plane.

The two sides also differ in their steric characteristics. As the phenyl groups lie above the plane, they form a steric pocket that can interact with potential ligands. This is particularly relevant to the Me_2BBZ complex since the axial ligand in pentacoordinate Me_2BBZ complexes also lies above the plane. Assuming that chiral Me_2BBZ complexes can be prepared, these steric features could be important for the use of these complexes in the chiral recognition of substrates. Below the plane, the benzimidazole groups and the puckering of the ligand forms more of a cavity. These latter features may be helpful for promoting regio- and stereoselective interactions that could be useful in catalytic processes.

Conclusion

Bis(benzimidazole)s represent a new class of macrocycle that exhibits distinct nonplanarities. The structures of this periodic series of metal−Me_2BBZ complexes demonstrate that metals can control the extent of these nonplanarities, with the basis for this control being the relative sizes of the metal ion and the Me_2BBZ metal-binding cavity. The ease by which the shape of these complexes can be altered provides further support for their potential utility in novel applications.

Acknowledgment. This work was partially supported by funds from The Ohio State University and the Hermann Frasch Foundation (Grant 416-HF97 to M.K.C.)

Supporting Information Available: Text and tables providing details of the structure determination and refinement, coordinates, anisotropic thermal parameters, and bond distances and angles and CIF data. This material is available free of charge via the Internet at http://pubs.acs.org.

IC991075A